

Investigation and dynamic analysis of a catastrophic rock avalanche on September 23, 1991, Zhaotong, China

Abstract At 6:10 p.m. on September 23, 1991, a catastrophic rock avalanche occurred in Zhaotong, Yunnan, southwestern China. Over 216 people were killed when the Touzhai village was overwhelmed directly in the path of the landslide. The landslide involved the failure of about 12 Mm³ of jointed basaltic rock mass from the source area. The displaced materials ran out a horizontal distance of 3650 m over a vertical distance of 960 m, equivalent to a Fahrböschung of 14.7°, and covered an area of 1.38 km². To provide information for hazard zonation of similar type of potential landslides in the same area, we used a dynamic model (DAN-W) with three alternative rheological models to simulate the runout behaviour of the displaced landslide materials and found that a combination of the frictional model and Voellmy model could provide the best performance in simulating this landslide. The simulated results indicated that the duration of the movement is estimated at about 175 s for a mean velocity 21 m/s.

Keywords Rock avalanche · Long runout · Dynamic analysis · DAN-W model

Introduction

Rock avalanches are triggered frequently by heavy rainfall, earthquake, and human activity and cause significant loss of human life and extreme damage to man-made structures and facilities in China (Wen et al. 2004; Huang 2009; Yin et al. 2009; Chigira et al. 2010; Dai et al. 2011; Yin 2011; Xu et al. 2014). Some giant rock avalanches with long runout distances are clearly extremely destructive, because they cannot be prevented and mitigated with usual civil engineering measures. The only possible and effective preventive and mitigating measure may be early warning and evacuation of vulnerable communities, which need some accurate understanding of the mechanism and dynamics of rock avalanches (Kilburn and Petley 2003). Therefore, the prediction of the character of the landslide, such as the possible velocity of the mass, the area of deposition, and the volume, is of great importance in landslide risk assessment. Many numerical studies have been performed to obtain a better understanding of landslides, and some rational approaches have been proposed for predicting the motion of landslide masses (e.g., Sassa 1988; Hungr 1995; Chen and Lee 2003; Crosta et al. 2003; Denlinger and Iverson 2004; McDougall and Hungr 2004, 2005; Poisel et al. 2008; Pirulli and Mangeney 2008; Huang et al. 2012; Pudasaini and Miller 2013; Pastor et al. 2014). Although the effectiveness of these approaches has been validated by back analyses of many landslides, successful forecasting of landslide movement has been rarely reported, because different models or parameters in these approaches should be used for differing types of landslides. However, back analyses of case histories are essential, because successful back analyses may be used to calibrate the models, improve forecasting accuracy, and also provide parameters specific to similar types of rapid landslides for use in the predictive modelling of potential landslides.

Permian basalt is widely distributed in Yunnan, Guizhou, and Sichuan of southwestern China, with an area of 30×10^4 km² and an

outcropping area of 37,538 km² (Shen et al. 2002). This type of rock usually results in a high-steep slope. Over the past several decades, two catastrophic basaltic rock avalanches (e.g., Touzhai landslide on September 23, 1991, and Lanni landslide on November 22, 1965) have caused significant casualties in Yunnan Province, southwestern China (Huang 2009; Xu and Huang 2010; Yin et al. 2013). Prevention and mitigation of these kinds of landslides are key issues in this area. Therefore, better understanding of the initiation and movement mechanisms and then forecasting the potential hazard area from these kinds of landslides are of great importance. By now, the investigation of actual cases of rock avalanches is a promising approach to obtain the unique knowledge of the potential disasters of rock avalanches in the mountainous areas with similar geoenvironments.

At 6:10 p.m. on September 23, 1991, a catastrophic landslide (located at latitude 27° 34′ 06.63″ N and longitude 103° 51′ 12.24″ E) occurred in Touzhai, Zhaotong, Yunnan, southwestern China (hereinafter called Touzhai landslide). The landslide devastated the village of Touzhai, killing 216 people, burying 202 houses and damaging 20 ha of farmland (Fig. 1).

In this paper, we selected the Touzhai landslide to better understand the runout behaviour of this type of landslide in the basalt distributed area. We summarized the main characteristics of the landslide and discuss its geological and climatic setting. We also analysed the runout behaviour of the landslide with the DAN-W model developed by Hungr (1995). We expect that these models and parameters could improve the accuracy of hazard assessment for those areas with their geological, topographical, and climatic features being similar to Touzhai landslide area.

Geological and climatic setting

The Touzhai landslide occurred in a region of high relief with a deeply incised valley. The Pan-he river, a tributary of Jinsha River, develops along a fault zone extending NE and has six branch valleys. The Touzhai valley is a branch of the Pan-he River and has a V-shaped cross section (Fig. 2). The valley is located on the left bank of the Pan-he River. The main valley has a length of 4 km and a drainage area of 3.6 km². The depth of the valley incision ranges from 300 to 1000 m, the longitudinal gradient of the valley bottom is 100 to 200‰, and the angle of the side slope is 25° to 70°. In the study area, Mount Yangjiaonao is located at the head of the valley and is the highest point with an elevation of 2850 m, and the Pan-he River is the lowest point with an elevation of 1820 m (Fig. 1b). The valley floor consists of seasonal alluvium and diluvium deposits. The vegetation is characterized by a discontinuous cover of low shrubs and little trees in the study area. The vegetation cover rates are 20–30 % in the valley and 35–50 % in other areas, respectively.

The exposed rocks in the study area (Fig. 6) are the five members of middle Permian basalt (P₂β), middle Permian sandstone and shale interbedded with a coal seam (P₂x), early Triassic sandstone and mudstone (T₁f), early Triassic sandstone and shale

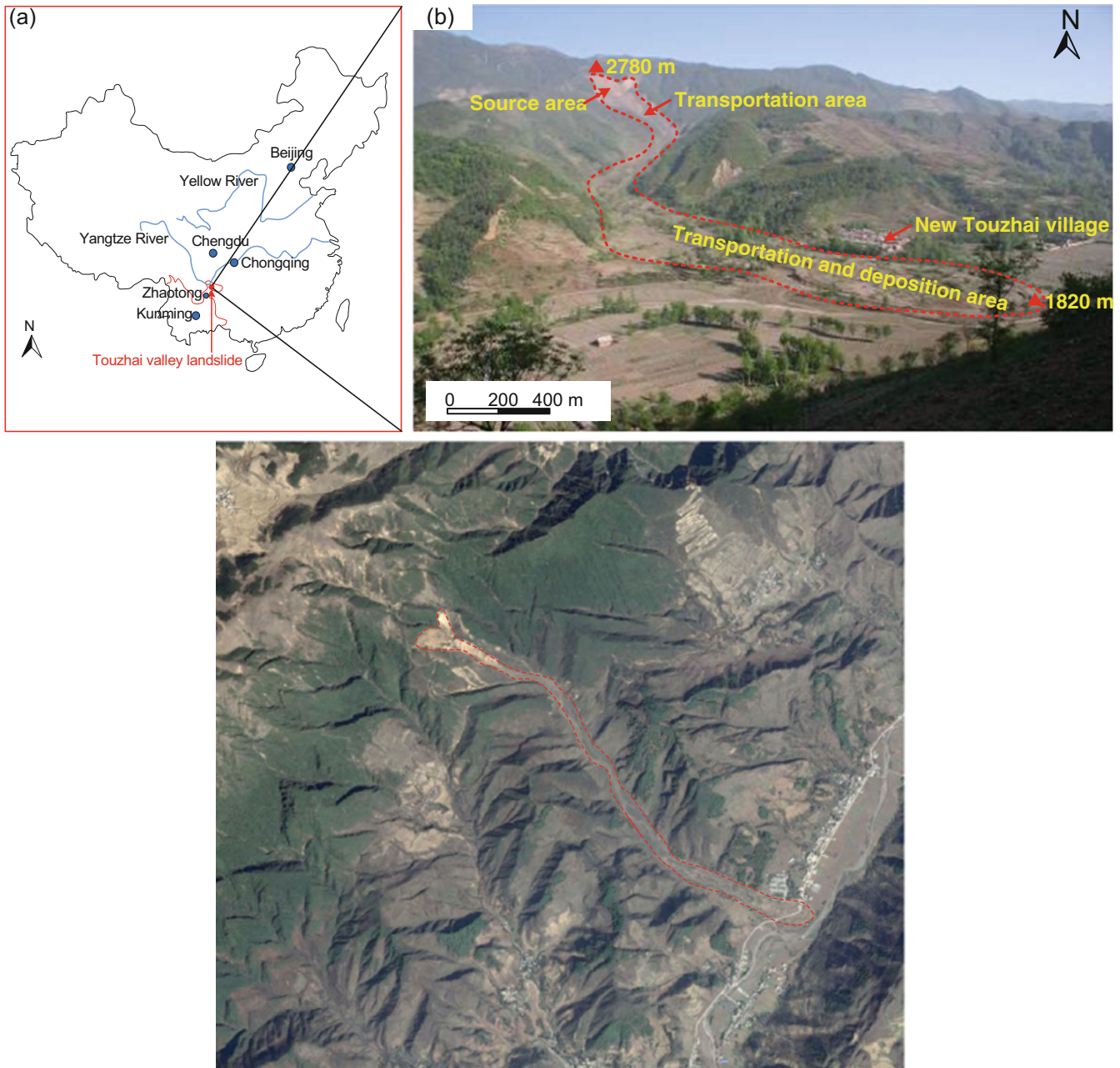


Fig. 1 a Location of the Touzhai valley landslide. b Overview of the Touzhai valley landslide taken in 2006. Two elevations are marked by red triangles. c A satellite image of the landslide from Google Earth on February 17, 2015

(T_{1y}), and Quaternary deposits (Q_{4al+pl}). A detailed description of the five members is further given in Table 1.

The study area is located in the southwestern part of the Yangzi Platform. The basic structural framework of the study area was formed due to the Yanshan tectonic uplift at the end of the Late Mesozoic Era and the regional plateau resulted from peneplanation by the end of the Miocene. At the beginning of the Pliocene, the fault block uplift was the major feature of the neotectonic movement at the study area. The geological structure of the study area consists of the Pan-he reverse fault, the Touzhai-Xindianzi syncline, and two joint sets, as a result of the second episode of the Himalayan movement (Fig. 3). The fault strikes 40° NE with a dip angle of 70° and the fault zone is 20 to 50 m in width.

The syncline is a linear-inclined syncline and has a distance of 1.1 km from the river. The axial line of the syncline is parallel to the fault strike. Its axial plane is nearly vertical and has a slight dip to SE. The core of the syncline is represented by the T_{1y} member, while its two limbs consist of the T_{1f} , P_{2x} , and $P_{2\beta}$ members. The northwestern limb of the syncline is wide and the southeastern limb is very narrow. It is cut by the Pan-he reverse fault which is not active at present.

The landslide area is located on the northwestern limb of the syncline. The rock mass in the source area contains two sets of joints (Fig. 4). The first set, a set of tension joints (J_1) approximately perpendicular to the Pan-he reverse fault, has a strike of 118° to 136° and a dip angle of 45° to 70° and a joint density of 1 to 5 per metre. The second, a



Fig. 2 Downstream view of Touzhai valley from the lower part of source area (taken in 1991). The location where this photo was taken is shown in Fig. 6

set of compressive joints (J₂), has a strike of 45°, a dip angle of 50°, and a joint density of 1 per metre. The second set develops along the original lava flow surface extending some tens of metres and dips to the free surface. The upper and middle parts of the slip surface are developed along the tension joint.

Xu et al. (2007) conducted a detailed study on the groundwater occurrence in this area and pointed out that the groundwater in the study area can be divided into three types: pore water in Quaternary loose deposits, bedrock fissure water, and carbonatite karst water in the deep layer. Pore water in the Quaternary loose deposits exists in loose sandy gravel layers along the two sides of the Touzhai valley and is mainly fed by rainfall. The groundwater runoff modulus of the aquifer is about 19.0 l/s/km².

Bedrock fissure water exists in the joints and weathering fissures of the clastic rock of Xuanwei Formation of Middle Permian and Early Triassic and the Emei Mountain basalt of Middle Permian. The aquifer of clastic rock is located at a depth of 20 to 50 m below the ground surface. The groundwater runoff modulus of the aquifer is about 2.0–3.0 l/s/km².

The basalt aquifer is located on a highly weathered belt with a depth greater than 50 m below the ground surface. The ground runoff modulus of the aquifer is about 3.0–5.0 l/s/km². The aquifer recharge is also from rainfall and it is sheet discharge for the aquifer. The groundwater in the landslide area belongs to the basalt fissure water. Water springs exist in the landslide area. The spring flow rate is usually 3 l/s and can be up to 500 l/s during a flood period (Tan 1993; Xu et al. 2007).

Carbonatite karst water mainly occurs in the limestone and dolomite layers of the Yongningzhen Formation of Triassic. The ground runoff modulus of the aquifer is greater than 15.0 l/s/km². The aquifer is mainly fed by rainfall and has a concentrated discharge area.

The study area has a humid semi-tropical monsoon climate. The annual average temperature is about 16.2 °C and ranges from 11.3 to 21.1 °C. January and July are the coldest and hottest months of the year, respectively. The annual average rainfall varies from 1090 to 1200 mm. Rainfall during the rainy season from May to October constitutes about 85.4 % of the total annual rainfall (Tan 1993). According to the Zhaotong and Yiliang Meteorology Stations records, cumulative rainfall values are respectively 99.0 and 39.3 mm from 11 to 23 September 1991. The maximum daily rainfall values of 43.0 and 11.0 mm were respectively recorded on September 16, 7 days before the occurrence of the landslide (Fig. 4).

Touzhai landslide

Post-failure behaviour and debris characteristics

The landslide involved a total volume of 15.0 Mm³. This included 12 Mm³ of jointed basaltic rock mass from the source area and 3 Mm³ of material entrained during transport. Of this total volume, 4.8 Mm³ deposited at the base of the source area while the rest deposited along the middle and lower sections of the valley (Fig. 5).

Based on a detailed field investigation, a geological map and a longitudinal profile of the Touzhai landslide are obtained and presented in Figs. 6 and 7, respectively. The landslide initiated as a rock slide in the large basalt rock mass with a strike 40° NE and a dip angle of 40° to 60°. After detaching from its source area, the slide mass ran down along the direction of 130°. After passing a corn field immediately below the source area, the slide mass encountered a lower ridge with a strike of 75° and a height of over 50 m at location R in Figs. 8 and 9a. The main part of the displaced

Table 1 Description of the rock formations in the study area

Rock formation	Description
P ₂ β	With a thickness over 350 m and mainly consisting of greyish-brown vesicular, compact, or amygdaloidal basalt interbedded with tuff. It outcrops at the head and upstream of the Touzhai Valley. The rock mass in the region is highly weathered and fractured, and has a granular or discrete structure resulting from long-term weathering and being dissected along primary and secondary joint planes.
P ₂ x	With a thickness of 77 to 194 m and consisting of yellow-grey medium to thin bedded with sandstone and shale interbedded with a coal seam.
T ₁ f	With a thickness of 252 to 652 m and consisting of highly weathered dark-purple medium to thick fine sandstone and siltstone interbedded with mudstone. It is mainly distributed at the middle and lower parts of the valley.
T ₁ y	With a thickness of 52 to 230 m and consisting of grey-red sandstone and shale in the upper part and limestone and dolomite in the lower part. It is distributed in the middle part of the valley.
Q ₄ al+pl	With a thickness of less than 30 m and mainly consisting of alluvial-pluvial deposits of sand, pebble gravel, and silty clay. It is distributed on the surface of the valley.

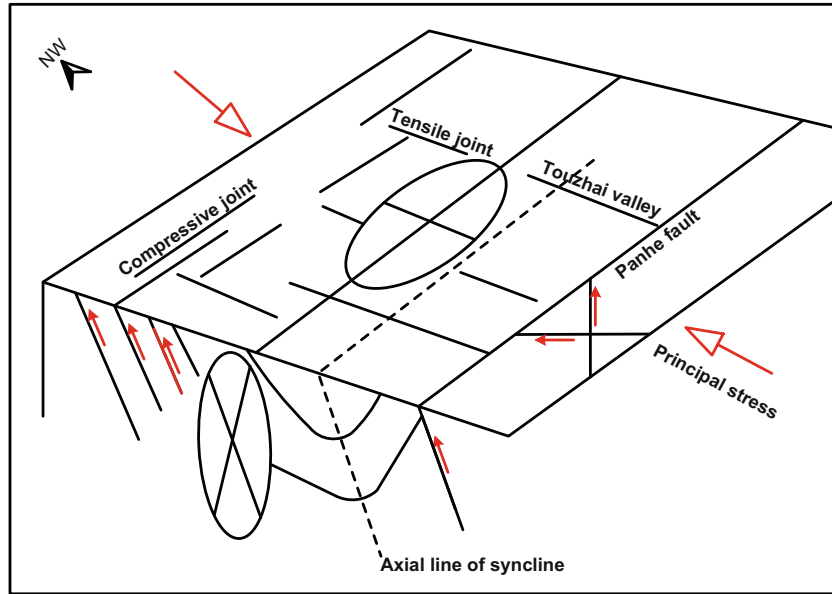


Fig. 3 Sketch of geological structure in the study area

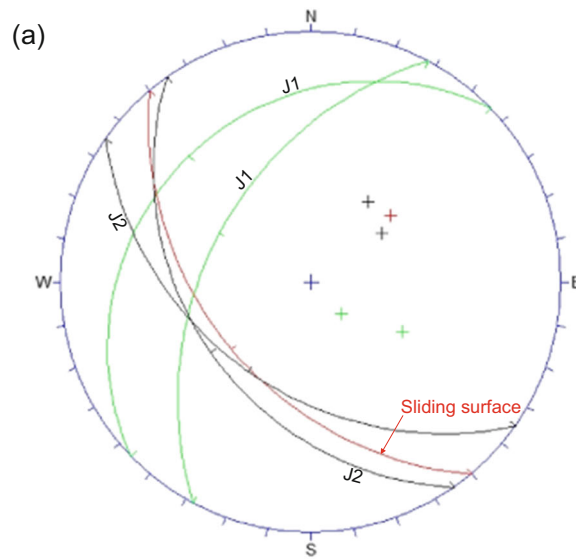


Fig. 4 a Stereonet graph of rock mass discontinuities in the source area (J_1 tension joints; J_2 compressive joints). b Fragmentized basaltic rock mass in the source area

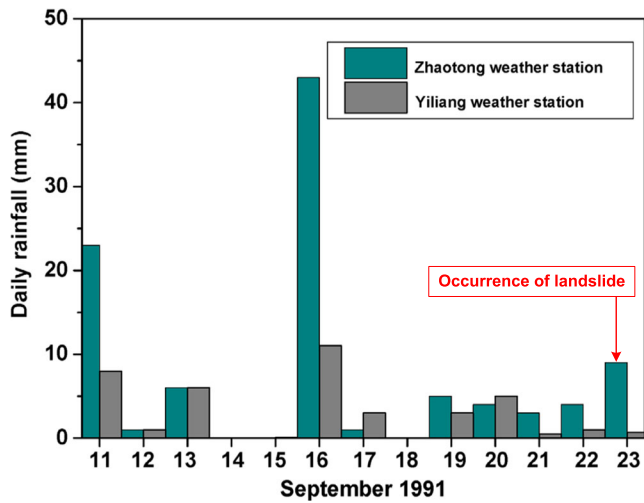


Fig. 5 Daily rainfall in the study area from September 11 to 23, 1991. Note that the landslide occurred 7 days after the peak rainfall on September 16

materials travelled toward the direction of 100° and superelevated on the left side of the valley at location T in Fig. 9a, and then fell back into the valley, continued to travel along the valley, and finally came to rest at the mouth of the valley (the residential area). Part of the materials impacted the side slope of the neighboring ridge and ran up this opposite slope to a maximum run-up height of 55 m at location S in Fig. 9a, and scattered rock debris and boulders on the back slope of the neighboring ridge (Fig. 9c). The displaced materials ran out a horizontal distance of about 3650 m with a descent of 960 m. It is noted that some houses, trees, and crops in the transportation and deposition areas had been damaged by the air blast, indicating rapid movement nature of the displaced materials (Fig. 10).

The source area is located on the eastern slope of Mount Yangjiaonao. The head scarp and the toe of the rupture surface are 2780 and 2300 m in elevation, respectively. The source area has a length of 900 m along the main slide direction, a width of 500 to 700 m, and an area of 0.49 km² (Figs. 6 and 11a). The slide mass mainly consisted of Permian basalt with a thickness of 5 to 120 m

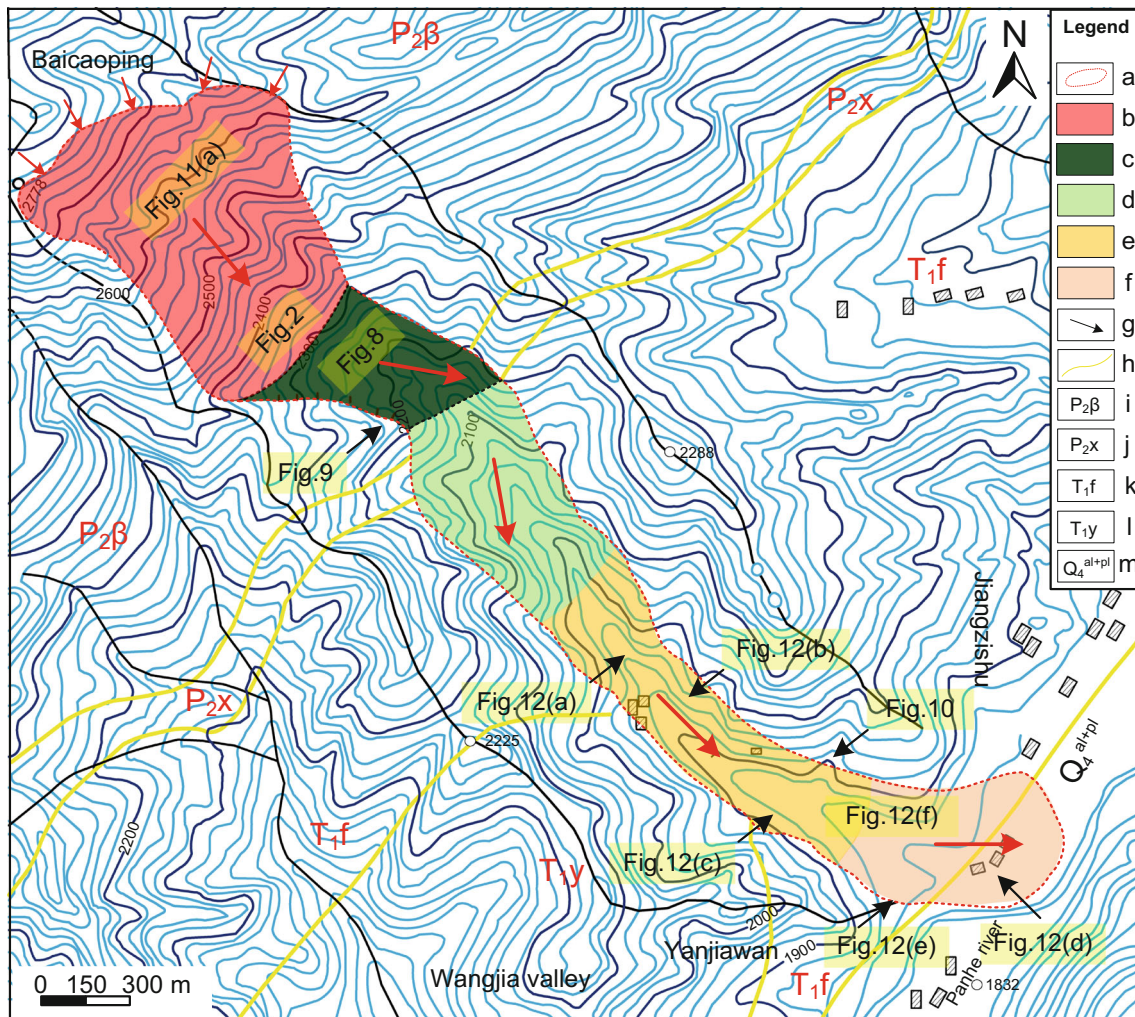


Fig. 6 Geological map of the Touzhai valley landslide. Legend: *a* Landslide boundary, *b* source area, *c* transportation area, *d* transportation and deposition area (zone I), *e* zone II, *f* zone III, *g* landslide direction, *h* stratigraphic boundary, *i* Permian basalt, *j* Permian sandstone and shale interbedded with coal seam, *k* Triassic sandstone and mudstone, *l* Triassic sandstone and shale, *m* Quaternary deposits

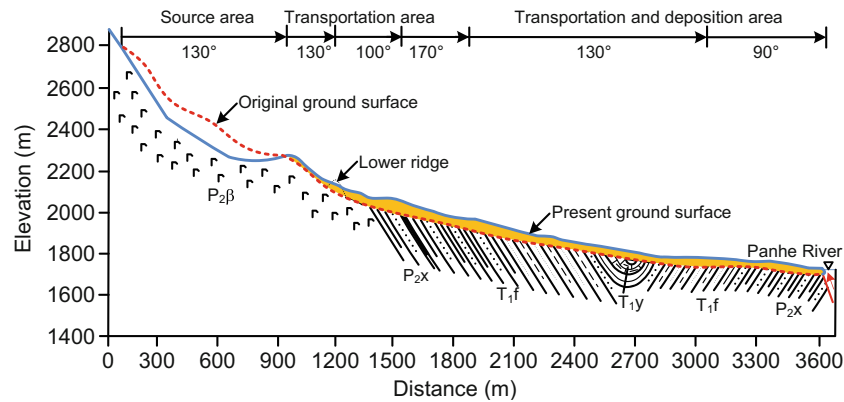


Fig. 7 Longitudinal profile of the Touzhai valley landslide along lines *a* and *b* shown in Fig. 6

and a volume of 12 Mm³. The double M-shaped head scarp has a width of 850 m along the direction of 27° NE and a slope angle of about 50°, and it is also the upper section of the rupture surface (Fig. 11b). The southwestern lateral scarp has a strike of 130° and a dip angle of 45°, and the northeastern lateral scarp has a strike of 150° and a dip angle of 80°. The rupture surface shows a shape with a steeper upper section and a gentle lower section. The upper and middle sections of the rupture surface have a dip of 130° and dip angles of 50° and 35°, respectively. The visible upper section of the rupture surface has a length of 550 m and an area of 0.3 km². The lower section of the rupture surface is concave upward shear plane with a length of 520 m and a strike of 35 to 40°. Field investigation revealed that the basalt rock mass was sheared along the lower section of the rupture surface prior to the landslide.

The transportation area extends a horizontal distance of 350 m from the toe of the rupture surface at an elevation of 2300 m to the valley floor at an elevation of 2120 m (Figs. 6 and 7). The area has a longitudinal length of 350 m and an area of 0.1 km². The secondary mudflow deposits in this area have a thickness of 3 to 5 m, a volume of 0.45 Mm³, and a longitudinal gradient of 25° to 28° (Fig. 8). The rock debris consists mainly of the basaltic rock ranging in size from 0.1 to 0.5 m and has a low content of clay matrix material.

The displaced materials mainly deposited at elevations ranging from 2120 to 1820 m. The transportation and deposition areas can



Fig. 8 Upstream view of secondary mudflow deposits in the transportation area

be divided into three subzones according to the elevation, direction of the landslide motion, and the longitudinal gradient of the deposits (Figs. 6 and 7).

Zone I is located at elevations ranging from 2120 to 1990 m (Fig. 9). This subzone has a longitudinal length of 750 m along the direction of 170°, an area of 0.26 km², an average thickness of about 25 m, and a volume of 6.5 Mm³. This subzone has a longitudinal gradient of 15° to 25°. The parent rock of the debris is composed mainly of basalt rock. About 85 % of the debris is rubble, 10 % gravel, and a small amount of purple-red sandstone and shale. The debris is relatively fine-grained materials in the middle part of the deposits and coarse-grained materials in both sides of the deposits.

Zone II is located at elevations ranging from 1990 to 1840 m. This subzone has a longitudinal length of 1000 m along the direction of 130°, an area of 0.25 km², a thickness of 10 to 15 m, and a volume of 2.6 Mm³. This subzone has a longitudinal gradient of 8° to 15°. There were multi-level transverse terrace scarps and sporadic knife-edge ridges with a height of 1 to 3 m, probably resulting from the tensile effect during the flow and deposition of rock debris (Fig. 12a). The deposits show a wave-like shape transverse cross-section and longitudinal ridges and furrows with a strike of 115° to 135° and can be found on both sides of the deposits (Fig. 12b). Coarse- and fine-grained materials display a band-shaped distribution in the same strike and generally forms some grooves at lateral margins. These sediments indicate both shearing and compressional faulting with the moving mass. The rock debris mainly consists of highly weathered rubble and gravel soils. In addition, the deposits of purple-red sandstone and shale show a band-shaped longitudinal distribution, probably due to the entrainment of materials from both side slopes (Fig. 12c).

Zone III is located at elevations ranging from 1840 to 1820 m. This subzone has a length of 500 to 570 m along the direction of 90°, a maximum width of 230 m, an area of 0.13 km², an average thickness of 5 m, and a volume of 1.1 Mm³. Touzhai village was buried by the rock debris in this subzone. Rock debris is composed mostly of basaltic rubbles and gravel soils. About 60 % of the rock debris was rubbles and gravels of basaltic rock and several large boulders (up to ~2 m in size) can also be seen in this subzone (Fig. 12e, f). Less than 10 % of the rock debris is rubbles and gravels of purple-red sandstone and shale. The micro-relief is characterized by hummocky and furrows-ridge reliefs with a height difference of 1 to 3 m and a strike of about 90° (Fig. 12d). The longitudinal axis of the micro-relief shows a radial spread near the Pan-he River.

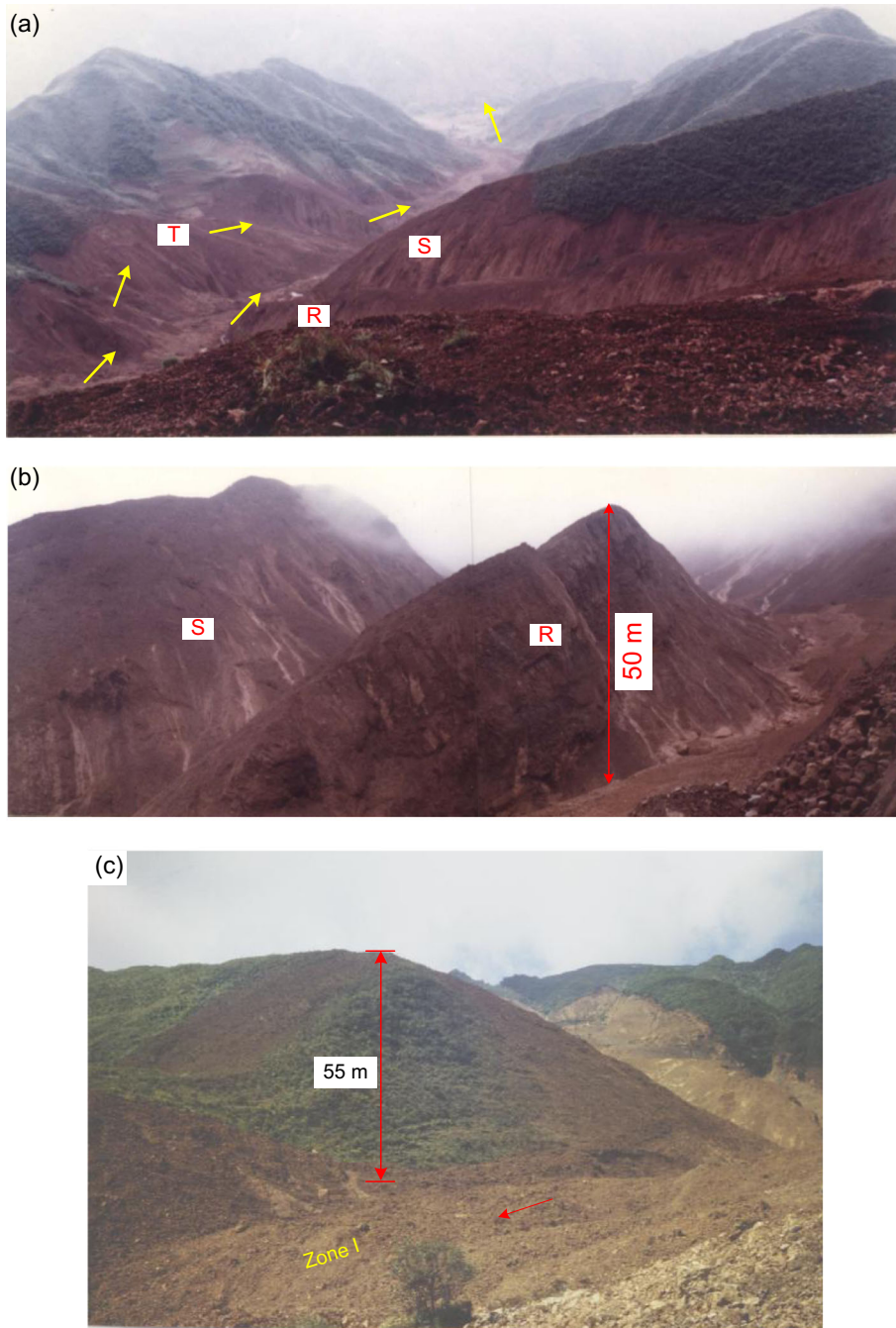


Fig. 9 Characteristics of the landslide after detaching from its source area. **a** The right flank of the slide mass flew over the lower ridge at location *R* and ran up the opposite slope of the other ridge at location *S*; its left flank superelevated on the left side of the valley at location *T*. **b** View of the two ridges toward the source area. **c** The slide mass scattered rock debris and boulders on the back slope of the other ridge

The trigger for the Touzhai landslide

Rock avalanches can be triggered by rainfall, earthquake, snow or glacier melting, and human activity. The occurrence of the Touzhai landslide is closely related to rock mechanical, geological, and environmental conditions including special geological structures, topography, and geomorphology.

In the late stage of Yanshan movement, the study area experienced strong tectonic movement and the principal compressive stress-oriented NW-SE (Fig. 3). This tectonic

movement laid a foundation for the present characteristics of geological structures and structural planes. Compressive and tensile structural planes are well developed in this study area. The compressive structural planes are parallel to the Pan-he fault and synclinal axial plane, and the tensile structural planes are perpendicular to the Pan-he fault. Compressive structural planes in basaltic rock are well developed from the original basalt flow surfaces on the northwestern flank of the syncline.

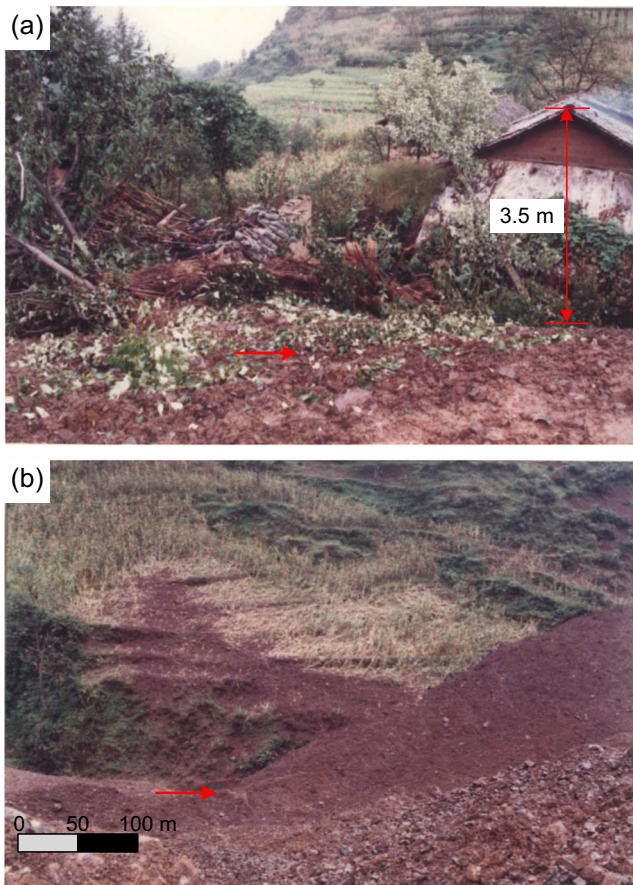


Fig. 10 a Air blast destroyed trees and houses and b flattened crops along the sides and front margin of the moving mass

Since the Cenozoic era, the study area has been experiencing the neotectonic movement of continuous uplifting. The neotectonic uplifting caused the deep cutting of Pan-he river basin and gradually evolved into the current alpine gorge geomorphology. The uplifting and down-cutting of the river also resulted in high and steep overhead side slopes. Major principal stresses along the NW-SE direction gradually disappeared and rebounded after unloading. As a result, the original compressive structural planes gradually changed into tensile structural planes. The compressive structural planes in the high and steep overhead side slopes and basalt rock mass of the landslide site are all parallel to the Pan-he River. The compressive structural planes developed from the basalt flow planes turned into tensile structural planes parallel to the side slopes. The tensile structural planes have good connectivity.

Meanwhile, due to the effect of severe uplifting and down-erosion, the basalt rock mass has a reduction of the vertical load and generated a group of nearly horizontal unloading fractures inside the rock mass. The horizontal unloading fractures evolved into shear structural planes at the toe area of the slope, oriented SE. Three groups of the structural planes severely cut the basalt rock mass in the study area. Consequently, the sliding surface, the side wall surfaces and the

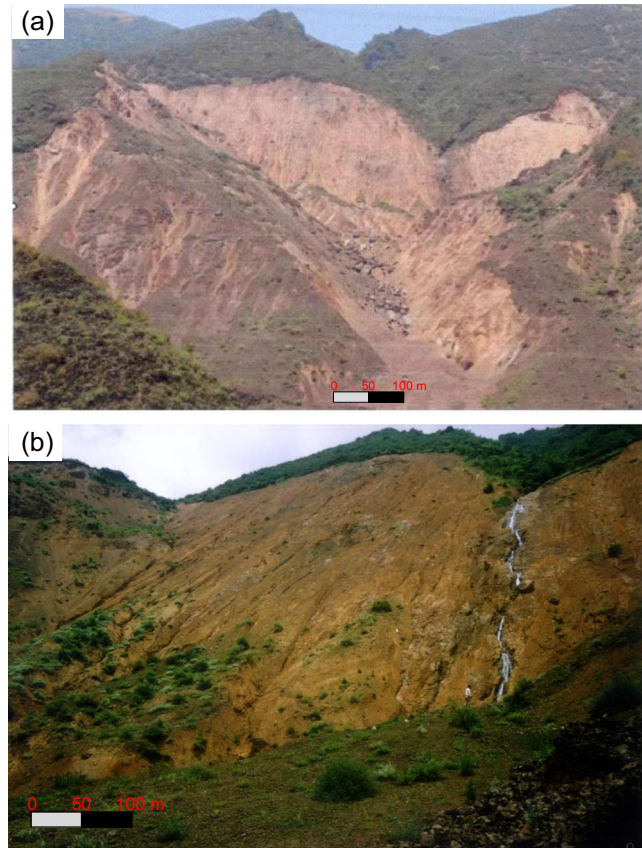


Fig. 11 a View of the source area and b head scarp of the landslide

outlet of shear plane of the landslide are controlled by the structural planes (Fig. 4).

Due to long-term weathering, network-like fissures are well developed throughout the basaltic rock mass. The weathered depth can be up to 80 m. The groundwater in the fissures made the basalt rock mass experience strong chemical weathering. The basalt rock mass has gradually softened and the shear strength of the rock structural planes has decreased.

Figure 12a shows the overview of the source area of the Touzhai landslide. The upper and middle parts of the slip surface was formed along the basaltic lava flow surface. The lower part of the near-horizontal slip surface was the locked segment of the slide mass.

A continuous rainfall occurred in the study area from September 11 to 23, 1991, and a large amount of surface runoff water directly penetrated into the upper and middle parts of the slip zones. In addition, perennial surface water runoff occurs in the head of the Touzhai valley. The water flow rate is usually 3 l/s during a dry season and may be up to 500 l/s during a flood period (Fig. 14). Such infiltration of runoff could cause a rapid rise in the level of the groundwater within the rock mass and saturate the slip zone soils. The rainfall could also increase the weight of the rock mass and soften the soils. As a result, the shear strength of the slip zone could be significantly decreased.

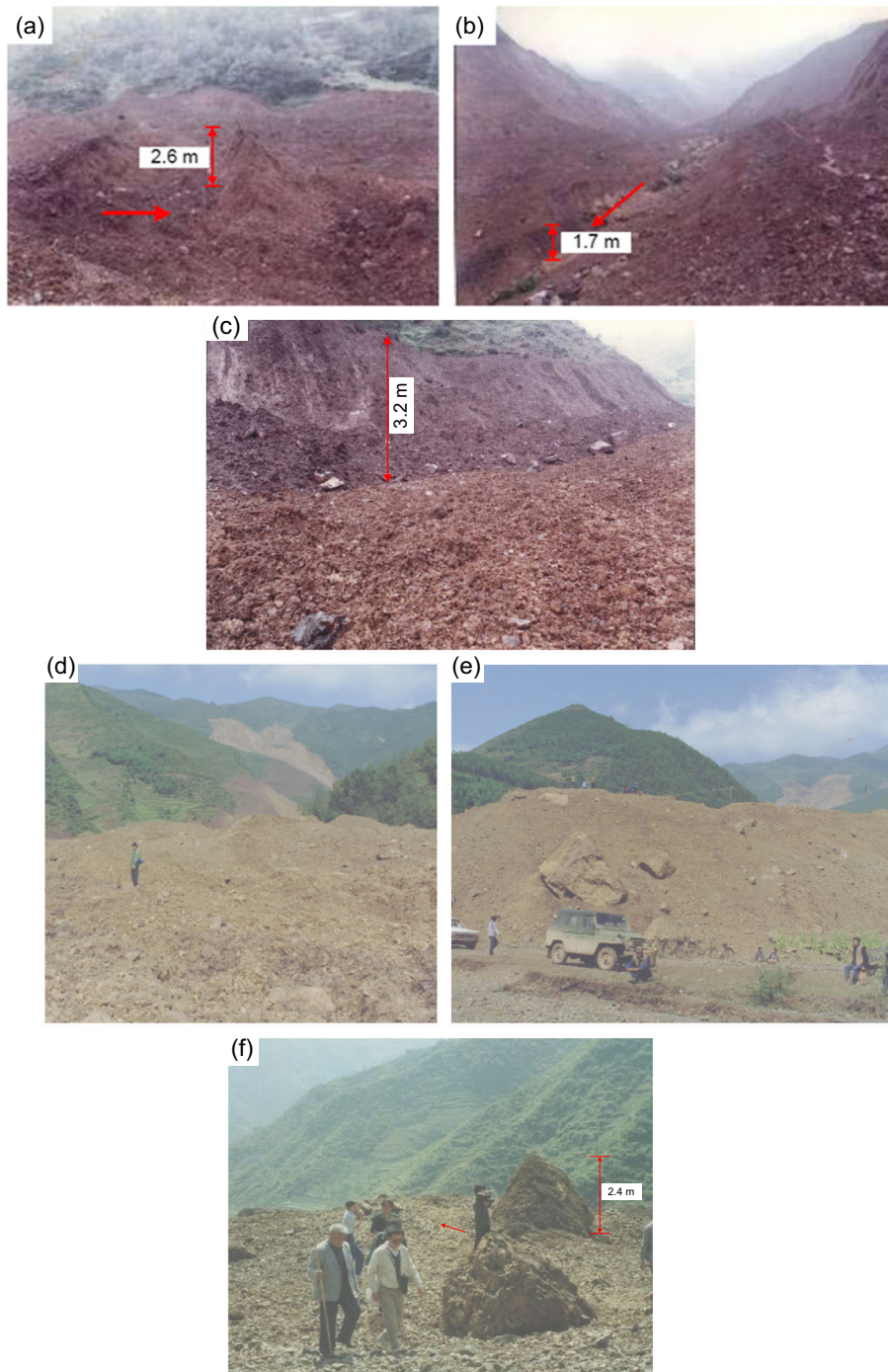


Fig. 12 Flow and deposition area. **a** Transverse ridges in zone II. **b** Longitudinal furrow in zone II. **c** Deposits resulting from the entrainment of lateral material. **d** Longitudinal ridges in zone III. **e** Distal deposits of the landslide. **f** Large boulders in zone III. The location of the photos is located in Fig. 6

Because the upper and middle slip surfaces were present, the above rock mass could produce some creep displacement and exert a driving force on the locked segment part. Once the shear stress exceeded the shear strength of the locked slip zone, the locked segment of the rock mass could suddenly rupture and result in the slide mass accelerating and sliding downward from the outlet of the shear plane along the direction of 130°. This sudden rupture of

the slip surface occurred at 6:10 p.m. on the evening of September 23, 1991.

Dynamic analysis

Dynamic model

To investigate the runout behaviour of the Touzhai landslide and provide parameters specific to the same type of

landslides for use in predictive modelling of potential landslides, a dynamic analysis of the landslide was performed using a two-dimensional model DAN-W (Hung 1995).

The dynamic model is governed by internal and basal rheological relationships. The rheologies that have been found to represent recorded events most accurately are the frictional and Voellmy rheologies (Boulton 2005). The frictional rheology assumes the resisting shear force (τ) to depend only on the effective normal stress (σ). The frictional equation is expressed as

$$\tau = \sigma(1-r_u)\tan\phi \quad (1)$$

where the pore pressure ratio, r_u , and the dynamic friction angle, ϕ , are the rheological parameters to be introduced in the model. The pore pressure ratio derives from the pore pressure, u , normalized by the total bed normal stress at the base, σ . The pore pressure ratio and the dynamic friction angle can be alternatively expressed by one single variable denoted as bulk basal friction angle, ϕ_b :

$$\phi_b = \arctan(1-r_u)\tan\phi \quad (2)$$

The Voellmy rheology describes the total resistance as a sum of a frictional and a turbulent term:

$$\tau = \sigma f + \rho g v^2 / \xi \quad (3)$$

The frictional term relates the shear stress to the normal stress through a friction coefficient, f , which is analogous to $\tan\phi_b$. The turbulent term summarizes all velocity-dependent factors of flow resistance and is expressed by the square of the velocity and the density of the debris through a turbulence coefficient, ξ .

Simulations of velocity were compared to the estimation of velocity from run-up and superelevation. Run-up velocity was measured using (Evans et al. 2001):

$$V_{\min} = (2gh)^{0.5} \quad (4)$$

where V_{\min} is the minimum velocity in metres per second, g is gravitational constant, and h is the run-up height.

Superelevation velocity was estimated by using (Evans et al. 2001)

$$V_{\min} = \left(gdr/b \right)^{0.5} \quad (5)$$

where V_{\min} is the minimum velocity in metres per second, g is gravitational constant, d is the superelevation, r is the radius of curvature in a bend, and b is the width of the path.

Influence of rheology and parameters

The initial failure geometry and travel path were specified as indicated in Fig. 7. The thickness of the various source zones were approximated by comparing the pre- and post-failure topography of the source area and identifying the main failure source. Data outside this zone were filtered, leaving a failed volume of approximately 12.0 Mm³. The identified source thickness were then subtracted from the pre-event topography to estimate the initial sliding surface elevations. Based on field measurements, we estimated that approximately 7.2 Mm³ of the sliding mass had been detached from the source area and 4.8 Mm³ of the basaltic rock mass was deposited in the lower part of the source area. Assuming a volume of 25 % volume bulking as suggested by Hung and Evans (2004), the total volume of displaced materials was estimated to be 9.0 Mm³. The volume of the displaced materials was increased by entrainment below the elevation of 2120 m. Our field estimate of the entrainment volume suggests an average erosion depth of 0.9 m equivalent to a yield rate of 500 m³/m along the travel path. Variable path widths were imposed according to the geological map of the landslide (Fig. 6).

Three alternative rheological models and parameters have been tried for the dynamic analysis of the Touzhai landslide (Table 2). The basal rheological parameters were adjusted by trial and error to achieve the best fit with the observed maximum runout distance, considering also published values from comparable case studies (Hung and Evans 1996; McDougall et al. 2006; Evans et al. 2007; Sosio et al. 2008). In all three cases, the model

Table 2 Back calculated values of the rheological parameters and models for the Touzhai valley landslide

	Rheology	ϕ (°)	r_u	f	ξ (m/s ²)
Model 1					
Source area	Frictional	15.0	0.6	–	–
Transportation area	Frictional	20.0	–	–	–
Transportation and deposition area	Voellmy	–	–	0.1	400
Model 2					
Source area	Voellmy	–	–	0.1	400
Transportation area	Voellmy	–	–	0.2	200
Transportation and deposition area	Voellmy	–	–	0.12	400
Model 3					
Source area	Frictional	20.0	0.6	–	–
Transportation area	Frictional	20.0	–	–	–
Transportation and deposition area	Frictional	16.0	0.4	–	–

parameters were adjusted so as to obtain the correct maximum runout distance. Figure 13 presents the results of the dynamic analysis using DAN-W with the above-selected rheological models and parameters. The results shows that the simulated deposit with the Voellmy model is thicker in the distal area than the field observation. The simulated deposit distribution with the frictional model is similar to that with the FFV model and agrees with the field observations. However, the simulated duration of the landslide with the FFV model is closer to the estimation from the seismic signal. Therefore, we selected a combined frictional-Voellmy model (FFV) to simulate the runout behaviour of the Touzhai landslide.

The frictional model can be used at the source area and transportation area and the Voellmy rheology at the flow and deposition areas. The transition between the frictional and Voellmy models was placed at an elevation of 2120 m. A dynamic friction angle of 30° was adopted for the frictional model, with pore pressure. We examined excess pore water pressure acting on the potential sliding surface at the source area because the sliding zone soil was fully saturated, equivalent to a range in pore pressure ratio (r_u) of 0.5 to 0.8, to simulate the frictional loss along the sliding surface resulting from the undrained loading. The dynamic friction angle of 20° was adopted for the frictional model at the transportation area without buildup of pore pressure. A Voellmy rheology was selected to characterize the runout behaviour of landslide below the elevation of 2120 m at the flow and deposition areas. For the simulation of this part of the path, values for the friction coefficient (f) in the range of 0.05–0.25 together with a range of values for the turbulence coefficient (ξ) of 400–500 m/s^2 were used. It is noted that these values for the Voellmy parameters are within the range of those found to best simulate the runout and velocity of the majority of rockslide-debris avalanche case histories analysed by Hungr and Evans (1996). These values were then used in a series of simulation runs to obtain the best fit for the observed characteristics of the Touzhai landslide.

Results and discussion

The results of the DAN-W simulation are presented in Fig. 14. Figure 14a shows the landslide profiles at different time steps

of the simulation. It can be seen that the duration of the movement is estimated at 175 s for an average velocity of 21 m/s. The results indicate that the calculated runout distance and deposit distribution correlate well with observations. Figure 14b shows the plot of velocity versus path distance. The maximum front velocity (49.9 m/s) occurred at a path distance of 1638 m. It is noted that the DAN-W simulation gave a sliding velocity of 47 m/s at location S and 26 m/s at location T in Fig. 2. At a path distance of 1250 m, the displaced mass flew over the lower ridge and ran up the opposite slope of the other ridge with a maximum run-up height of 55 m at location S in Fig. 2, and Eq. (4) yields a velocity estimate of 33 m/s for a measured run-up of $h=55$ m. At a path distance of 1800 m, the debris entered a major bend at location T in Fig. 2. For this bend, Eq. (5) yields a velocity of 29.7 m/s for the parameters of $d=60$, $r=300$, and $b=200$ m. The locations and estimated velocities are superimposed in Fig. 14b. Although there are some differences in the velocities obtained by differing methods, we concluded that DAN-W simulation gave a promising prediction of the sliding velocity for this landslide. Figure 14c shows the plot of average deposit thickness along path. The final distribution of the debris given by the simulation shows that the maximum debris thickness obtained in the simulation is 64 m at a path distance of 670 m (Fig. 14c), which shows a good agreement with the data estimated from field investigation. As a result of the limitation of the DAN-W model, the debris thickness of the simulation in zone III is much larger than that of field observation. As mentioned above, the residual deposits have a volume of 4.8 Mm^3 in the lower part of the source area. The simulated result with the FFV model gave a runout distance of 3604 m, slightly less than the observed case of 3650 m (Fig. 14c), a reduction of 1.3 %.

Based on the DAN-W model, a large number of case studies of rapidly moving landslides in North America have been analysed and a valuable database of calibrated parameters has been created (cf. Hungr et al. 2005). Further case studies will be performed using the DAN-W model to obtain the travel distance and velocity of the same type of rapid landslides for conducting landslide hazard assessment in the mountainous areas of southwestern China.

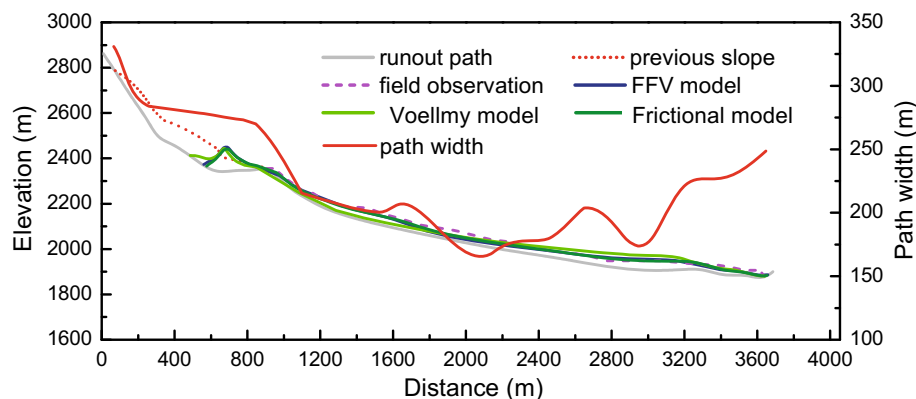


Fig. 13 Comparison of the final deposit profiles from different rheological models

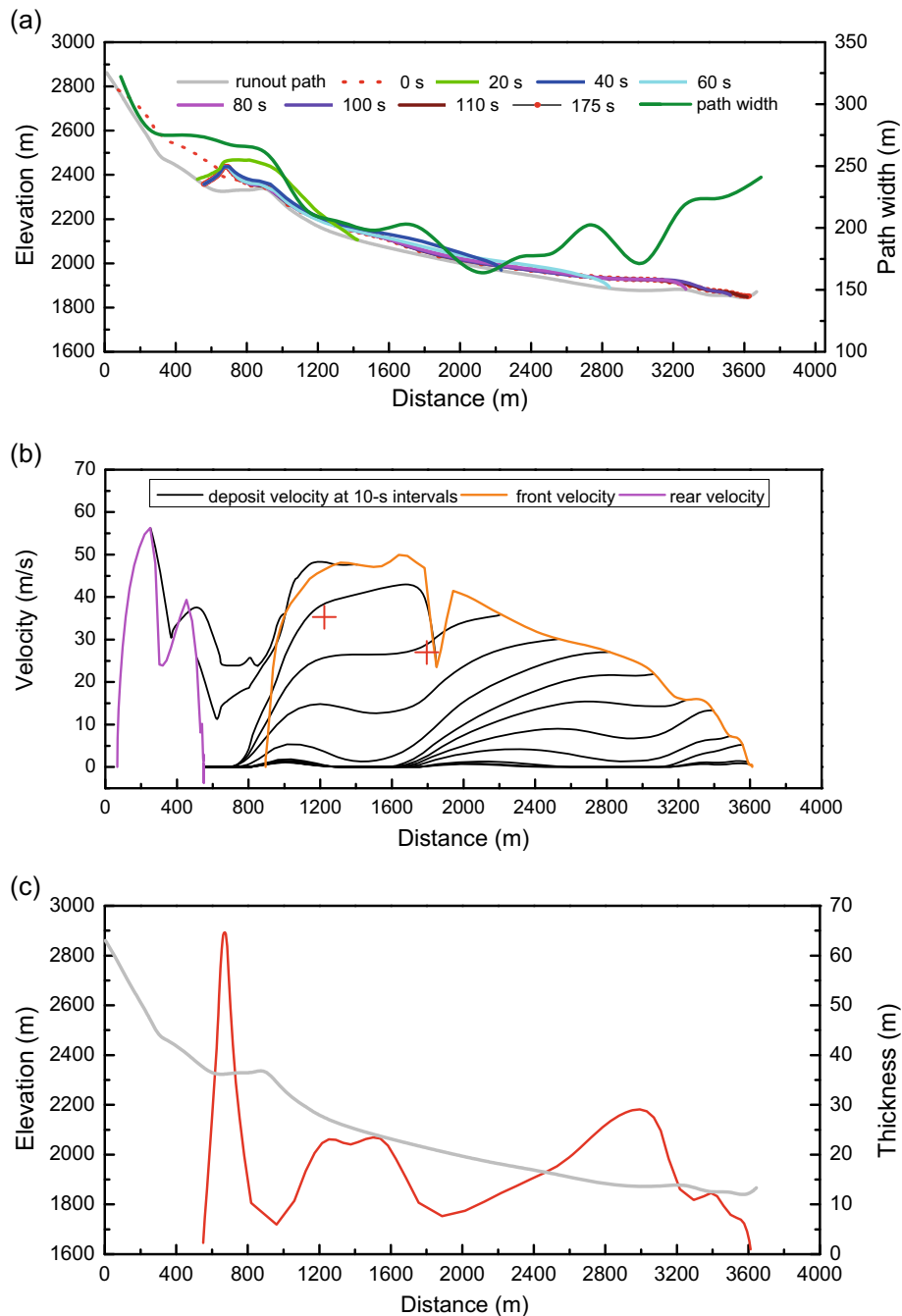


Fig. 14 Simulated results for the Touzhai valley landslide. **a** Landslide profiles at different time steps of the simulation; path width from the topographical map. **b** Plot of velocity versus path distance. Velocities are compared to estimates from superelevation and run-up data (*red cross*). **c** Plot of deposit thickness versus path distance

Conclusions

On September 23, 1991, a catastrophic landslide occurred in Zhaotong, Guizhou, China. In this paper, we introduced the setting and main characteristics based on the field investigation and analysed the runout behaviour with the DAN-W model. Some conclusions are made as follows.

- (1) The occurrence of the Touzhai landslide is closely related to rock mechanical, geological, and environmental conditions including special geological structures, topography, and geomorphology.
- (2) The landslide travelled a maximum horizontal distance of over 3600 m with a maximum vertical descent of 960 m. Its debris destroyed the village of Touzhai and killed 206 people. The displaced landslide materials created an air blast in the transportation and deposition areas, damaging houses, trees, and crops along the travel path, highlighting the rapid movement nature of the landslide.
- (3) The DAN-W model was used to simulate the runout process, and the results showed that a combined FFV (Frictional-Frictional-Voellmy) model provides the best performance in simulating this landslide. The total duration of the landslide

was 175 s with an average velocity of 21 m/s. Very good agreement between the observed and simulated results was achieved, suggesting that this model with the parameters obtained through back analyses could be a strong tool for the prediction of landsliding in the same area, and then to the similar type of landslide hazard.

Acknowledgments

This study was supported by the National Natural Science Foundation of China (No. 41272382 and 41372332) and National Science Fund for Distinguished Young Scholars (No. 41225011). We are grateful to Prof. O. Hungr for supplying a copy of the DAN-W software.

References

- Boulton N (2005) Characterization of the Zymoetz River rock avalanche. M.Sc. thesis, Simon Fraser University, Burnaby
- Chen H, Lee CF (2003) A dynamic model for rainfall-induced landslides on natural slopes. *Geomorphology* 51(4):269–288
- Chigira M, Wu XY, Inokuchi T, Wang GH (2010) Landslides induced by the 2008 Wenchuan earthquake, Sichuan, China. *Geomorphology* 118(3–4):225–238
- Crosta GB, Imposimato S, Roddeman DG (2003) Numerical modelling of large landslides stability and runout. *Nat Hazards Earth Syst Sci* 3(6):523–538
- Dai FC, Tu XB, Xu C, Gong QM, Yao X (2011) Rock avalanches triggered by oblique-thrusting during the 12 May 2008 Ms 8.0 Wenchuan earthquake, China. *Geomorphology* 132(3–4):300–318
- Denlinger RP, Iverson RM (2004) Granular avalanches across irregular three-dimensional terrain: 1. Theory and computation. *J Geophys Res Earth Surf* 109(F1):1–14
- Evans SG, Hungr O, Clague JJ (2001) Dynamics of the 1984 rock avalanche and associated distal debris flow on Mount Cayley, British Columbia, Canada; implications for landslide hazard assessment on dissected volcanoes. *Eng Geol* 61:29–51
- Evans SG, Guthrie RH, Roberts NJ, Bishop NF (2007) The disastrous 17 February 2006 rockslide-debris avalanche on Leyte Island, Philippines: a catastrophic landslide in tropical mountain terrain. *Nat Hazards Earth Syst Sci* 7:89–101
- Huang RQ (2009) Some catastrophic landslides since the twentieth century in the southwest of China. *Landslides* 6:69–81
- Huang Y, Zhang WJ, Xu Q, Xie P, Hao L (2012) Run-out analysis of flow-like landslides triggered by the Ms 8.0 2008 Wenchuan earthquake using smoothed particle hydrodynamics. *Landslides* 9(2):275–283
- Hungr O (1995) A model for the runout analysis of rapid flow slides, debris flows, and avalanches. *Can Geotech J* 32(4):610–623
- Hungr O, Evans SG (1996) Rock avalanche run out prediction using a dynamic model. In: Senneset (ed.) *Landslide Proc Int Symp Trondheim* 1:33–238
- Hungr O, Evans SG (2004) Entrainment of debris in rock avalanches: an analysis of a long run-out. *Geol Soc Am Bull* 116(9–10):1240–1252
- Hungr O, McDougall S, Bovis M (2005) Entrainment of material by debris flows. In: Jakob H (ed) *Debris flow hazards and related phenomena*. Springer, Heidelberg, pp 135–158
- Kilburn CRJ, Petley DN (2003) Forecasting giant, catastrophic slope collapse: lessons from Vajont, Northern Italy. *Geomorphology* 54:21–32
- McDougall S, Hungr O (2004) A model for the analysis of rapid landslide motion across three-dimensional terrain. *Can Geotech J* 41(6):1084–1097
- McDougall S, Hungr O (2005) Dynamic modelling of entrainment in rapid landslides. *Can Geotech J* 42(5):1437–1448
- McDougall S, Boulton N, Hungr O, Stead D, Schwab JW (2006) The Zymoetz River landslide, British Columbia, Canada: description and dynamic analysis of a rock slide-debris flow. *Landslides* 3:195–204
- Pastor M, Blanc T, Haddad B, Petrone S, Sanchez Morales M, Drempevic V, Issler D, Crosta GB, Cascini L, Sorbino G, Cuomo S (2014) Application of a SPH depth-integrated model to landslide run-out analysis. *Landslides* 11:793–812
- Pirulli M, Mangeney A (2008) Results of back-analysis of the propagation of rock avalanches as a function of the assumed rheology. *Rock Mech Rock Eng* 41(1):59–84
- Poisel R, Preh A, Hungr O (2008) Run out of landslides—continuum mechanics versus discontinuum mechanics models. *Geomech Tunne* 1(5):358–366
- Pudasaini SP, Miller SA (2013) The hypermobility of huge landslides and avalanches. *Eng Geol* 157:124–132
- Sassa K (1988) Geotechnical model for the motion of landslides. In: *Proc. 5th International Symposium on Landslides, “Landslides”*, Balkema, Rotterdam, vol.1. pp 37–56
- Shen JH, Wang LS, Li TB, Zhao QH (2002) Structural characteristics of basaltic rock masses in Southwestern Sichuan, China. *J Chengdu Univ Technol* 29(6):680–685
- Sosio R, Crosta GB, Hungr O (2008) Complete dynamic modeling calibration for the Thurwieser rock avalanche (Italian Central Alps). *Eng Geol* 100(1–2):11–26
- Tan JZ (1993) Discussion on the motion characteristics of the Touzhai landslide. *Geol Hazards Environ Preserv* 4(1):37–43
- Wen BP, Wang EZ, Wang SJ, Zhang JM (2004) Characteristics of rapid giant landslides in China. *Landslides* 1:247–261
- Xu ZM, Huang RQ (2010) The geological structure constraint for massive and catastrophic landslides in Permian Emeishan basalt. *Geol Rev* 56(2):224–236 (in Chinese)
- Xu ZM, Huang RQ, Tang ZG (2007) Engineering geological characteristics of the Touzhai Landslide and its occurrence mechanisms. *Geol Rev* 53(5):691–698 (in Chinese)
- Xu C, Xu XW, Yao X, Dai FC (2014) Three (nearly) complete inventories of landslides triggered by the May 12, 2008 Wenchuan Mw 7.9 earthquake of China and their spatial distribution statistical analysis. *Landslides* 11(3):441–461
- Yin YP (2011) Recent catastrophic landslides and mitigation in China. *J Rock Mech Geotech Eng* 3(1):10–18
- Yin YP, Wang FW, Sun P (2009) Landslide hazards triggered by the 2008 Wenchuan earthquake, Sichuan, China. *Landslides* 6(2):139–152
- Yin YP, Liu CZ, Chen HQ, Ren J, Zhu CB (2013) Investigation on catastrophic landslide of January 11, 2013 at Zhaojiagou, Zhenxiong County, Yunnan Province. *J Eng Geol* 21(1):6–15 (in Chinese)

A. Xing

State Key Laboratory of Ocean Engineering, Shanghai Jiao Tong University, Shanghai, 200240, China
e-mail: xingaiquo@sjtu.edu.cn

G. Wang

Research Center on Landslides, Disaster Prevention Research Institute, Kyoto University, Uji, 611-0011, Japan

Y. Yin

China Institute of Geo-Environment Monitoring, Beijing, 100081, China

C. Tang · W. Li

State Key Laboratory of Geohazard Prevention and Geoenvironment Protection, Chengdu University of Technology, Chengdu, 610059, China

Z. Xu

Department of Civil Engineering, Kunming University of Science and Technology, Kunming, 650224, China